Biophysical Journal Volume 71 July 1996 227–236

Impaired Slow Inactivation in Mutant Sodium Channels

Theodore R. Cummins and Frederick J. Sigworth
Interdepartmental Neuroscience Program and Department of Cellular and Molecular Physiology, Yale University School of Medicine, New Haven, Connecticut 06520 USA

ABSTRACT Hyperkalemic periodic paralysis (HyperPP) is a disorder in which current through Na^+ channels causes a prolonged depolarization of skeletal muscle fibers, resulting in membrane inexcitability and muscle paralysis. Although HyperPP mutations can enhance persistent sodium currents, unaltered slow inactivation would effectively eliminate any sustained currents through the mutant channels. We now report that rat skeletal muscle channels containing the mutation T698M, which corresponds to the human T704M HyperPP mutation, recover very quickly from prolonged depolarizations. Even after holding at −20 mV for 20 min, ~25% of the maximal sodium current is available subsequent to a 10-ms hyperpolarization (−100 mV). Under the same conditions, recovery is less than 3% in wild-type channels and in the F1304Q mutant, which has impaired fast inactivation. This effect of the T698M mutation on slow inactivation, in combination with its effects on activation, is expected to result in persistent currents such as that seen in HyperPP muscle.

INTRODUCTION

Hyperkalemic periodic paralysis (HyperPP) is a rare autosomal dominant muscle disorder that afflicts humans (Streib, 1987). Skeletal muscle fibers biopsied from individuals with HyperPP have a tetrodotoxin-sensitive persistent current that activates at potentials more negative than the threshold for normal sodium channels (Lehmann-Horn et al., 1983, 1987). This persistent current leads to an enhanced depolarization in HyperPP muscle that results in paralysis under some circumstances (Ricker et al., 1989).

Several distinct mutations have been identified in the adult skeletal muscle sodium channel gene of families with HyperPP, paramyotonia congenita, or other forms of myotonia (Barchi, 1995). The effects of these mutations are difficult to isolate in native muscle tissue, so many groups have studied mutations in mammalian expression systems, using either HEK-293 cells or TsA201 cells, a transformed variant of the HEK-293 cells. The α subunit of the adult skeletal muscle sodium channel produces sodium currents in HEK-293 cells that appear to be identical to those found in native muscle fibers (Ukomadu et al., 1992). It is therefore believed that the properties of mutant channels will also be very similar in HEK-293 and native muscle cells.

The most common HyperPP mutation is the T704M mutation (Ptacek et al., 1991; Rüdel et al., 1993). Three different groups studied this mutation, using transient transfection techniques to express the channels. Cannon and Strittmatter (1993) and Cummins et al. (1993) both studied the HyperPP-T704M mutation by making the corresponding mutation in the rat skeletal muscle sodium channel (rT698M), and Yang et al. (1994) studied the HyperPP-T704M in the human skeletal muscle channel (hT704M). In these studies two different mechanisms were proposed to underlie the persistent current.

Cummins et al. (1993) found that the voltage dependence of activation was shifted by −12 mV for rT698M channels relative to wild-type rat μI (WT) channels. This shift increases the amount of overlap between the activation and steady-state inactivation processes, which can result in "window" currents between −75 and −40 mV. This is the voltage range where persistent sodium currents are observed in HyperPP muscle fibers and could account for the slightly increased depolarization (−57 mV compared with −63 mV for control muscle) that elevated extracellular potassium induces in HyperPP fibers (Lehmann-Horn et al., 1987). Yang et al. (1994), working with the hT704M human channel, also concluded that window currents could be important in HyperPP pathophysiology.

Alternatively, Cannon and Strittmatter (1993) proposed that noninactivating current, resulting from failure of normal fast inactivation, underlies the persistent current. Indeed, in all three expression studies the mutant channels yielded a larger noninactivating component of the sodium current elicited by large depolarizations. Cannon and Strittmatter reported that cells transfected with the rT698M mutant channel exhibited a large noninactivating component, nearly 10% of the peak current, at voltages in the normal activation range.

Although either of these mechanisms leads to persistent currents that could theoretically induce muscle depolarization and paralysis, neither can account for the prolonged paralysis lasting several hours in patients with HyperPP (Rüdel and Lehmann-Horn, 1985). Ruff (1994) contends that without an impairment of sodium channel slow inactivation, muscle function would recover much more quickly than is observed. This is because any channels giving rise to persistent currents would enter the slow-inactivated state

Received for publication 29 February 1996 and in final form 18 April 1996.

Address reprint requests to Dr. F. J. Sigworth, Department of Cellular and Molecular Physiology, Yale University School of Medicine, 333 Cedar Street, New Haven, CT 06520. Tel.: 203-785-5773; Fax: 203-785-4591; E-mail: fred.sigworth@yale.edu.

0006-3495/96/07/227/10 $2.00

within minutes and stop conducting, thus allowing the muscle membrane potential (and muscle function) to recover.

Slow-inactivation processes have been described in several nerve and muscle preparations. During prolonged depolarizations sodium channels enter inactivated states from which recovery is very slow, often taking several minutes (Almers et al., 1983; Kirsch and Anderson, 1986; Ruben et al., 1992; Rudy, 1978; Simoncini and Stühmer, 1987). Slow inactivation is thought to be kinetically and functionally distinct from the fast-inactivation process, first described by Hodgkin and Huxley (1952), which occurs on a time scale of milliseconds. It appears to be a separate voltage-dependent process that provides long-term modulation of sodium channel availability.

In view of the critical role that slow inactivation may have in muscle excitability and HyperPP pathophysiology, we thought it important to characterize slow inactivation in channels that have the HyperPP-T704M mutation.

MATERIALS AND METHODS

Expression system

The generation of the rT698M mutant was described previously (Cummins et al., 1993). In that study WT and rT698M cDNAs were assembled in the mammalian expression vector pRBG4 (Ukomadu et al., 1992). We removed a 5922 bp fragment containing either the WT or rT698M cDNA from this vector, using EcoRI, and subcloned it into another mammalian expression vector, pJB20, which contains the neomycin resistance gene as well as the cytomegalovirus immediate early promoter/enhancer. The new constructs were screened for the presence (rT698M) or absence (WT) of a unique BstEII site as well as being mapped with several other restriction enzymes.

The WT-pJB20 and rT698M-pJB20 constructs were introduced into HEK-293 cells by the calcium phosphate precipitation technique (Ukomadu et al. 1992). HEK-293 cells were grown in high-glucose Dulbecco's modified Eagle medium (Gibco, Gaithersburg, NY) supplemented with 10% fetal calf serum (FCS; Gibco). After 48 h, antibiotic (Geneticin, Gibco) was added to select for cells expressing the neomycin resistance. After 2–3 weeks colonies were picked and subsequently tested for channel expression by whole-cell recording techniques. We screened 12 independent colonies for WT currents and 9 independent colonies for rT698M currents. Six of twelve WT lines expressed a significant amount of current in the initial screening (peak current average of 1.4 ± 0.7 nA, mean ± SD, for the six lines, 5–6 cells from each line). Five of nine rT698M lines expressed a significant amount of current in the initial screening (peak current average of 474 ± 131 pA for the five lines, 5–6 cells from each line). The two highest-expressing WT lines and rT698M lines were used for experiments. Cells were split and grown in Dulbecco's modified Eagle medium, with no added FCS or antibiotics for 2–3 days before recording. We have found that when the cells are grown for 2–5 days in the absence of FCS and antibiotics the peak current for both WT and rT698M currents is 200–400% larger, although the basic current properties are not significantly affected (data not shown).

Whole-cell recordings

We conducted whole-cell patch-clamp recordings at room temperature (~22°C), using an EPC-9 amplifier. Data were acquired on a Macintosh IIci computer with the Pulse program (v. 7.52, HEKA Electronic, Lambrecht, Germany). We fabricated fire-polished electrodes (0.8–1.5 MΩ) from 1.5-mm Kimax capillary glass, using a Sutter P-87 puller (Novato, CA). To minimize space-clamp problems and because HEK-293 cells can be electrically coupled, only isolated cells with a soma size of 10–30 μm were selected for recording. The average cell capacitance was 17 ± 5 pF (n = 31) for rT698M cells and 18 ± 6 pF (n = 30) for WT cells. Cells were not considered for analysis if the initial seal resistance was less than 5 GΩ, they had high leakage currents (holding current >0.1 nA at −80 mV), membrane blebs, or an access resistance greater than 3 MΩ. Access resistance was monitored throughout the experiment, and data were not used if resistance changes occurred. The average access resistance was 1.8 ± 0.3 MΩ (n = 31) for rT698M cells and 1.9 ± 0.4 MΩ (n = 30) for WT cells. Voltage errors were minimized by 80% series resistance compensation, and the capacitance artifact was canceled by the computer-controlled circuitry of the patch-clamp amplifier. The average peak current was 16 ± 9 nA for WT cells and 9 ± 8 nA for rT698M cells. These peak current values are not necessarily representative of the respective populations because cells at either extreme have been excluded from the data: WT cells with very large currents (>30 nA) were not used because of clamping problems, and rT698M cells with small currents (<1 nA) were not used in an effort to avoid contamination by endogenous HEK-293 currents (Cummins et al. 1993). The estimated peak voltage error, after compensation, was 6 ± 4 mV for WT cells and 3 ± 3 mV for rT698M cells used in this study. Linear leak subtraction, based on resistance estimates from 4–5 hyperpolarizing pulses applied before the depolarizing test potential, was used for all voltage-clamp recordings. Membrane currents were filtered at 5 kHz and sampled at 20 kHz. The pipette solution contained 140 mM CsF, 2 mM $MgCl_2$, 1 EGTA, 10 mM glucose, and 10 mM Na-HEPES (pH 7.3). The standard bathing solution was 140 mM NaCl, 3 mM KCl, 2 mM $MgCl_2$, 2 mM $CaCl_2$, 10 mM HEPES, and 10 mM glucose (pH 7.3). The liquid junction potential for these solutions was <5 mV; data were not corrected to account for this offset. The osmolarity of all solutions was adjusted to 310 mosM (Wescor 5500 osmometer, Logan, UT). The offset potential was zeroed before the cells were patched and checked after each recording for drift: if the drift was greater than 5 mV/h the recording was not used.

Cell-attached recordings

As a control, some macroscopic currents were measured from cell-attached patches. For these experiments the cell membrane potential was zeroed by use of a high K^+ bathing solution (150 mM potassium aspartate, 5 mM KCl, 4 mM $MgCl_2$, 2 mM $CaCl_2$, 10 mM HEPES [pH 7.3]), and the pipette solution contained a high Na^+ solution (150 mM NaCl, 3 mM KCl, 2 mM $MgCl_2$, 2 mM $CaCl_2$, 10 mM HEPES [pH 7.3]).

Data analysis

We analyzed data on a Macintosh computer, using Pulsefit (v. 7.52), or on a 486-PC, using custom software developed by one of the authors, T.R.C. Statistical analysis was done with the Systat program, and statistical significance was determined by $p < 0.05$ by the unpaired t-test. Analysis results are expressed as mean ± SD. The curves in the figures are drawn to guide the eye unless otherwise noted, and the error bars in the figures represent standard errors. Steady-state inactivation curves were fitted to the Boltzmann function

$$\frac{I}{I_{peak}} = \frac{1}{1 + \exp\left(\frac{V - V_h}{k}\right)},$$

where I_{peak} is the peak current measured, V_h is the midpoint of the curve, and k is the slope factor.

RESULTS

Characterization of stable cell lines

The present study made use of HEK-293 cell lines stably expressing the WT sodium channel and the rT698M mutant. The properties of channels expressed in these cells were similar to those that we observed previously in transiently

transfected cells (Cummins et al., 1993). The magnitude of the shift in activation and the relative size of the persistent current were generally consistent, and, as with the transient transfections, the current density was significantly smaller for rT698M cells (530 ± 440 pA/pF; mean ± SD, $n = 31$) than for WT cells (920 ± 520 pA/pF; $n = 30$ for WT; $p = 0.003$). However, with the recording conditions used here for studying slow inactivation, there are some differences from what we previously reported (Cummins et al. 1993). When initially establishing whole-cell recordings, we often observed larger persistent currents (both window and non-inactivating currents). However, during the first 10 min after establishing whole-cell recordings we generally observed a decrease in the size of the persistent current, an increase in the size of the peak current, and apparent shifts in the activation and steady-state inactivation curves. Because the protocols used to measure slow inactivation required fairly long recordings, in the experiments reported here cells were always allowed to stabilize for 20 min before we acquired data to minimize the unwanted effects of time-dependent drifts. With fluoride as the main anion, we were able to maintain stable whole-cell recordings with low access resistances and low leak currents for as long as 4 h. Under these conditions the noninactivating current components were consistently small for both WT and rT698M channels (typically less than 0.5%; see Fig. 1 *A* and *B*).

Tests for slow inactivation

Slow inactivation is thought to be distinct from fast inactivation in both its kinetics and voltage dependence. The voltage dependence of the steady-state slow inactivation is reflected by the channel availability variable s_∞; in rat and human skeletal muscle the s_∞ curve has a more negative midpoint voltage than the h_∞ curve (Simoncini and Stühmer, 1987; Ruff et al., 1987; Ruff and Whittlesey, 1992). In rat fast-twitch muscle Simoncini and Stühmer (1987) used 20-ms prepulses to estimate that the midpoint voltage V_h of the h_∞ curve was near −80 mV. By changing the membrane potential for longer durations they estimated that the midpoint of the s_∞ curve (V_s) was −108 mV. Because fast inactivation is complete within 30–50 ms for skeletal muscle sodium channels, increasing the length of the inactivating prepulse beyond 50 ms should not increase the amount of fast inactivation. But, if slow inactivation occurs at more negative voltages than fast inactivation, further increases in the duration of the inactivating prepulse will allow slow inactivation processes to predominate, and the sodium channel availability curve will reflect slow inactivation. Similarly, Fahlke and Rüdel (1992) reported that increasing the duration of the inactivating prepulse from 20 to 500 ms shifts the availability curve of human myoballs by ~−20 mV.

To test for an effect of this kind, we measured currents following prepulse durations of 50, 500, 5000, and 50,000 ms (Table 1). As shown in Fig. 1 *C* and *D*, there is only a slight difference between the inactivation curves obtained with 50-ms and with 50-s prepulse durations. The midpoint of inactivation (V_h) was shifted by less than 5 mV in the negative direction by the longer prepulses for both WT and rT698M channels. This result suggests that slow inactivation for the rat channel expressed in HEK-293 cells occurs

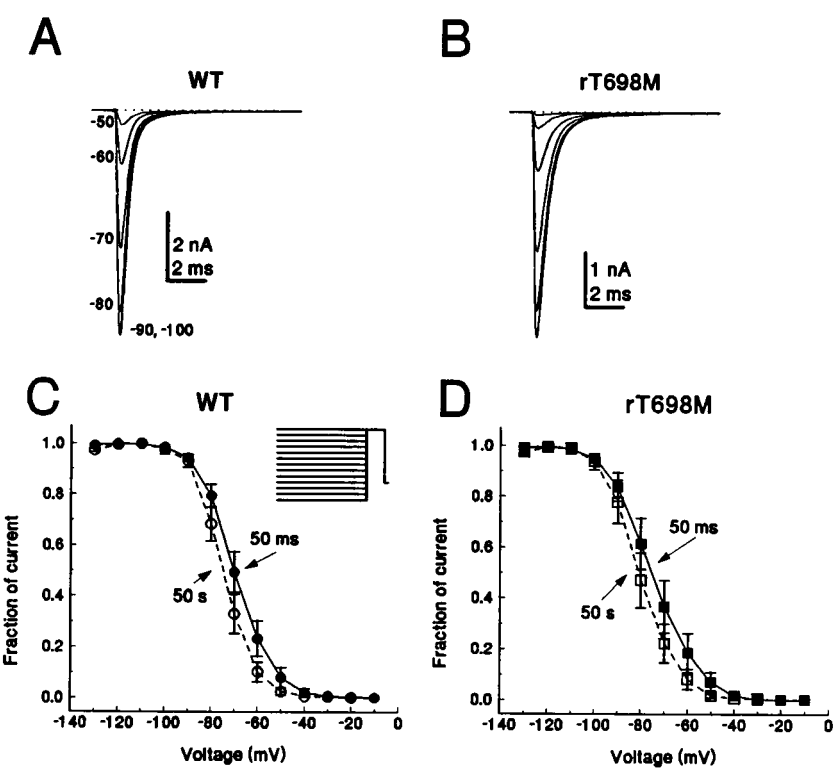

FIGURE 1 Effect of prepulse duration on steady-state inactivation for rT698M and WT currents. (*A* and *B*) Family of traces from representative HEK-293 cells expressing either WT (*A*) or rT698M (*B*) channels. The currents were elicited by test pulses to −10 mV after 50-ms prepulses to various potentials (−100, −90, −80, −70, −60, and −50 mV). (*C*) The steady-state inactivation (h_∞) curves for WT channels with 50-ms (●, *solid curve*, $n = 7$) and 50-s (○, dashed curve, $n = 7$) inactivating prepulses are shown. (*D*) The h_∞ curves for rT698M channels with 50-ms (■, *solid curve*, $n = 7$) and 50-s (□, *dashed curve*, $n = 7$) inactivating prepulses are shown. Cells were held at prepulse potentials over the range of −130 to +10 mV before a test pulse to −10 mV for 20 ms (*inset* shown in *C*). Current is plotted as a fraction of peak current. As a control for drift in the h_∞ curve over time, a second 50-ms h_∞ curve was recorded after the initial set of curves was obtained (typically 24 min after the first 50-ms curve). The V_h value for the second curve was on average 3 mV more negative than V_h for the first 50-ms curve. This trend suggests that the underlying difference in V_h between the 50-ms and the 50-s h_∞ curves might actually be smaller than the 5-mV difference indicated in (*C*) and (*D*) and in Table 1.

TABLE 1 Effect of prepulse duration on steady-state inactivation parameters

Prepulse Duration	WT (mV)		rT698M (mV)	
	V_h	k	V_h	k
50 ms	−69.5 ± 6.4	6.8 ± 0.5	−75.0 ± 8.4	7.7 ± 1.4
500 ms	−71.8 ± 5.1	6.4 ± 0.4	−77.4 ± 7.6	7.0 ± 0.8
5 s	−73.1 ± 5.1	6.1 ± 0.4	−78.9 ± 7.4	6.8 ± 0.9
50 s	−74.5 ± 5.4	5.8 ± 0.6	−80.2 ± 7.5	6.5 ± 0.9
	$n = 7$		$n = 6$	

at more positive voltages than fast inactivation, if it occurs at all.

To determine better whether the sodium currents expressed in HEK-293 cells have a slow inactivation process, we needed to study channels that were not in the fast-inactivated state. Because channels recover from fast inactivation within several milliseconds, short hyperpolarizing recovery pulses can be used to remove fast inactivation just before a test pulse to measure slow-inactivation processes. Hyperpolarizing recovery pulse durations of 20–80 ms were used to characterize slow inactivation in rabbit (Kirsch and Anderson, 1986), rat (Simoncini and Stühmer, 1987), and human (Ruff and Whittlesey, 1992) skeletal muscle fibers. By using this type of protocol, we are able to compare slow inactivation in HEK-293 cells with what is known about slow inactivation in skeletal muscle fibers from previous studies. Initially we chose a recovery pulse of 10 ms to −100 mV, which is sufficient to remove 80–90% of fast inactivation in WT and rT698M channels (Cummins et al., 1993).

Results from two slow-inactivation experiments are shown in Fig. 2. Cells were held at a given potential for 5 min, during which, every 15 s, a 10-ms recovery pulse to −100 mV was applied followed by a 20-ms test pulse to −10 mV. The 20-ms test pulse duration was chosen because it allows the characterization of the full time course of fast inactivation. Using this protocol, we observed a voltage-dependent slow-inactivation process that occurs in both WT (Fig. 2 *A*) and rT698M (Fig. 2 *B*). Slow inactivation appeared incomplete in cells expressing rT698M channels (Fig. 2*C* and *D*). This incomplete inactivation was observed in several cells, but, because the test sequence is time consuming, it was difficult to get a complete measure of the voltage dependence of slow inactivation on a large number of cells in this way.

Voltage dependence of slow inactivation

To allow a larger number of observations to be made, we used a sequential protocol to estimate the voltage dependence of s_∞. In this protocol the cells were held at various holding potentials, starting at −130 mV, for 50 s; a 10-ms, −100-mV recovery pulse and a 20-ms test pulse (to −10 mV) followed each 50-s dwell at the holding potential. The holding potential

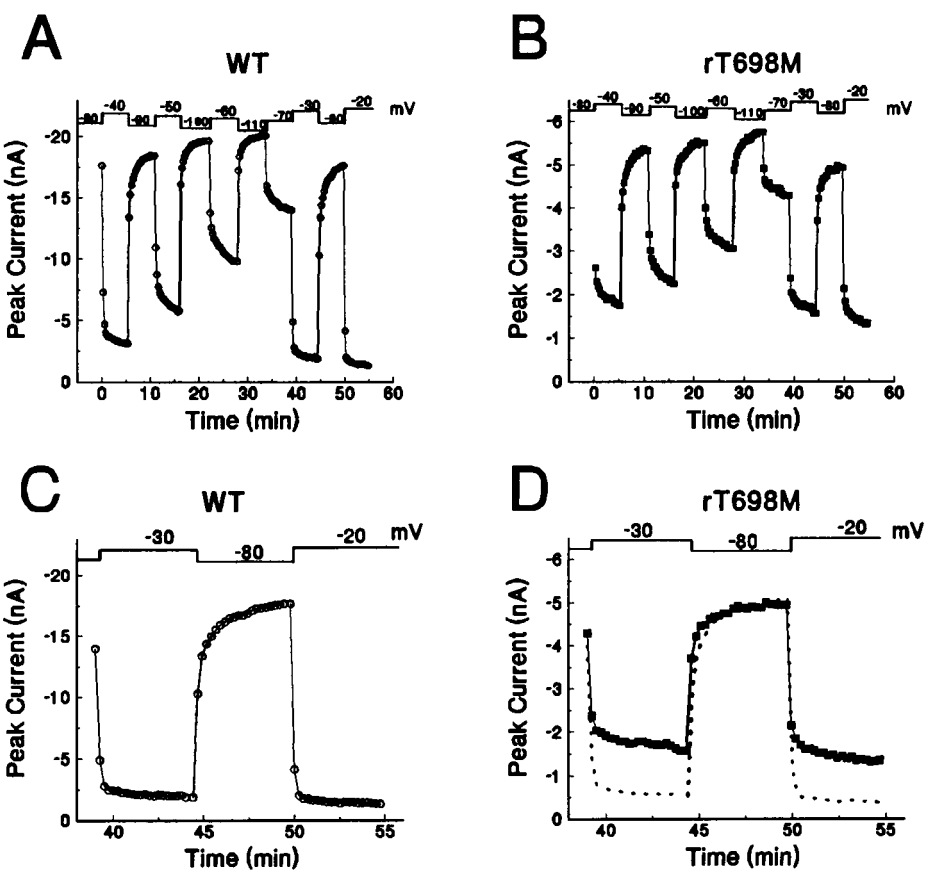

FIGURE 2 Slow inactivation in rT698M cells and WT cells. (*A* and *B*) Changes in peak sodium current for a representative WT cell (*A*) and an rT698M cell (*B*) in response to changes in the holding potential. Cells were allowed to stabilize for 20 min at −80 mV before the test protocol was begun. The protocol involved holding the cell at a specific potential for 5 min while once every 15 s the membrane potential was stepped to −100 mV for 10 ms, then to 0 mV for 20 ms. The peak current elicited by the test pulse to 0 mV is plotted. In (*C*) and (*D*) the data from the last three holding potentials in (*A*) and (*B*) are shown on an expanded time scale. The holding potential sequence is shown at the top of each panel. For comparison, the data from (*C*) are also shown (*dotted curve* in *D*) after the maximum current has been normalized. Slow inactivation appears to be less fully developed in rT698M cells.

was then incremented by 10 mV after each recovery pulse/test pulse sequence. We term this protocol sequential because the channels are not allowed to recover from slow inactivation for each test pulse; the hope is that the sequential changes in holding potential will mimic changes in holding potential of longer durations. For WT channels this protocol yielded an s_∞ curve (Fig. 3 *A*) that can be well fitted by a Boltzmann function; however, for rT698M channels we again observed a significant impairment of slow inactivation (Fig. 3 *B*). At −20 mV, 25 ± 9% (n = 18) of the rT698M channels are available for activation after only a 10-ms recovery pulse, compared with 4 ± 2% (n = 16) for WT channels (Fig. 3 *A*). As a check of the sequential protocol, the peak current amplitude measured after 5 min at each different holding potential (data from Fig. 2 *A* and *B*) is shown superimposed upon the 50-s s_∞ curves in Fig. 3 *A* and *B*. The correspondence between the two protocols is excellent.

As can be seen from Fig. 2 *D*, development of slow inactivation seems more gradual for rT698M than for WT channels, which raises the possibility that rT698M channels simply inactivate more slowly than WT channels. On a step from −100 to −20 mV the time constant measured from 5 s to 5 min was much shorter for WT channels (8 ± 4 s, n = 10) than for rT698M channels (61 ± 19 s, n = 12). Thus the possibility arises that the incomplete slow inactivation seen in Fig. 2 *D* might be artifactual, caused by dwell times that were too short.

To address the possibility that the development of slow inactivation in rT698M cells would go to completion if allowed enough time, we subjected several rT698M and WT cells to a sequential slow-inactivation protocol with a 300-s dwell time at each holding potential. Given a time constant of 61 s, the 300-s holding pulse should allow more than 99% of the rT698M channels to enter the slow-inactivated state at each holding potential. As it turns out, the 300-s s_∞ curves (Fig. 3 *C*) differ little from the corresponding curves obtained with the 50-s s_∞ protocol, and V_s values for WT channels measured with 300-s holding pulses were not statistically different from those measured with 50-s holding pulses in the same cells. With the 300-s protocol a significant difference, however, remains between the WT and rT698M curves. At −20 mV, 3 ± 2% (n = 3) of the WT channels were available for activation after the 10-ms hyperpolarizing recovery pulse, compared with 20 ± 10% (n = 3) of the rT698M channels. This shows that slow inactivation in rT698M channels is not simply slower but also appears to be incomplete.

A 10-ms recovery pulse is relatively brief, allowing only ~80% recovery from fast inactivation, which has a time constant of 8 ms at −100 mV. Therefore the effect of varying the duration of the recovery pulse was also examined. The 50-s sequential s_∞ protocol was used with 30- and 105-ms recovery pulses instead of the 10-ms pulse previously used. For WT channels (Fig. 4 *A*) there was no difference between the results obtained with 10- and 30-ms recovery pulses. With the 105-ms recovery pulse the WT s_∞ values increased to ~0.1 at positive voltages, but the midpoint voltage was not significantly changed. For rT698M channels (Fig. 4 *B*) the s_∞ curves become shallower with the increasing duration recovery pulses, and none of the curves could be fitted with a Boltzmann function. With a holding pulse potential of −20 mV, 39 ± 10% (n = 6) of the channels were available after a 30-ms recovery pulse and 46 ± 12% (n = 7) were available after a 105-ms recovery pulse.

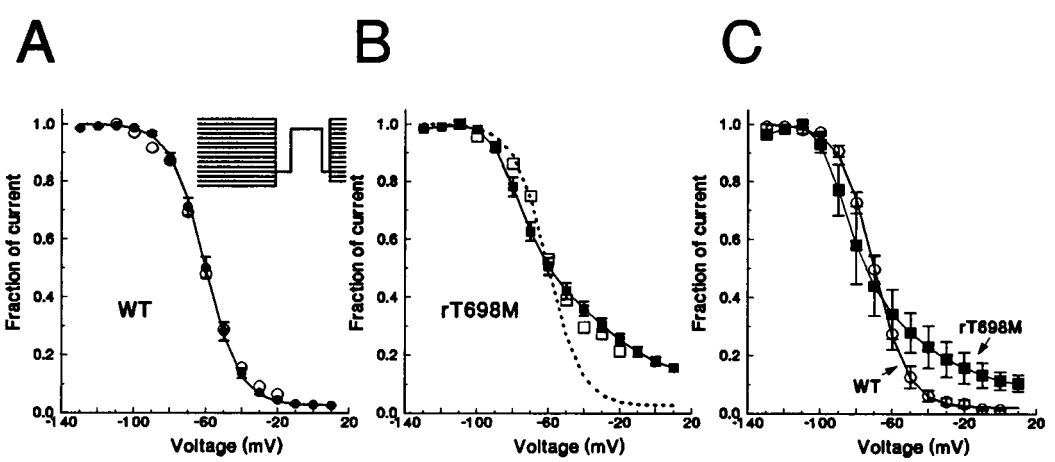

FIGURE 3 Steady-state slow-inactivation curves. The steady-state slow inactivation (s_∞) curves for WT (*A*) and rT698M (*B*) cells are shown. Cells were held at potentials starting from −130 mV and increasing to +10 mV in 10-mV steps. After 50 s at each holding potential, a 10-ms recovery pulse to −100 mV and a 20-ms test pulse to −10 mV were given before the holding potential was incremented. The peak current elicited by the test pulse to −10 mV is plotted as a fraction of the maximum current for WT cells (*A*, ●, n = 16) and rT698M cells (*B*, ■, n = 18). The solid curve in (*A*) is a Boltzmann fit to the data, where V_s = −60.5 ± 6.1 mV and k = 9.4 ± 1.4 mV (n = 16). In (*A*) the data from the last test pulse for each different holding potential in Fig. 2 *A* are also plotted (○). The solid curve in (*B*) is drawn to guide the eye. Also in (*B*) the data from the last test pulse at each different holding potential in Fig. 2 *B* are plotted (□) as well as the s_∞ curve for WT cells from (*A*) (*dotted curve*). The value of s_∞ remains large even at positive potentials, indicating that slow inactivation is impaired in rT698M cells. (*C*) Sequential slow-inactivation curves as in (*A*) and (*B*), except with 300-s dwell at each holding potential. The peak current elicited by the test pulse to −10 mV is plotted as a fraction of the maximum current for WT cells (○, n = 3) and rT698M cells (■, n = 3). The WT, but not the rT698M, s_∞ curve was well fitted with a Boltzmann function (V_s = −70.3 mV, k = 9.3).

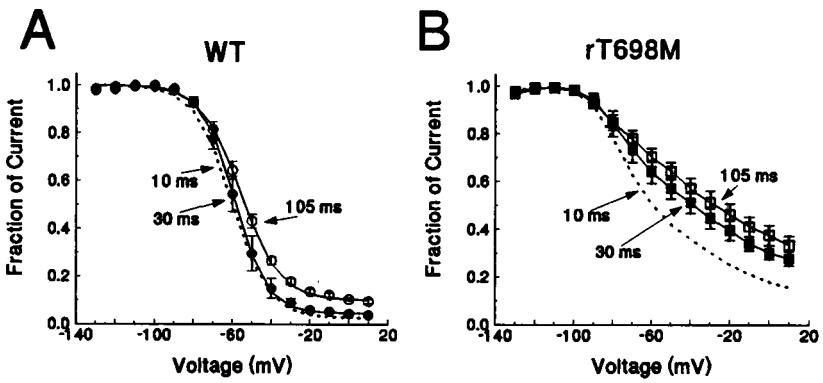

FIGURE 4 Effect of recovery pulse duration on the s_∞ curve. (*A* and *B*) Effect of increasing the recovery pulse duration on the WT (*A*) and the rT698M (*B*) s_∞ curves. Cells were held sequentially at potentials from −130 to +10 mV for 50 s before a 30-ms (●, ■) or a 105-ms (○, □) recovery pulse to −100 mV and a 20-ms test pulse to −10 mV. The dotted curve in (*A*) is the WT data from Fig. 3 *A* (10-ms prepulse), and the dotted curve in (*B*) is from Fig. 3 *B* (10-ms prepulse). Increasing the recovery pulse duration has little effect on the WT s_∞ (*A*) but makes the rT698M s_∞ curve shallower and less well developed (*B*). The WT 30- and 105-ms s_∞ curves were fitted with a Boltzmann function: for the 30-ms s_∞ curve V_s is −59 ± 5 mV and k is 8.4 ± 0.8 (mean ± SD, n = 4); for the 105-ms curve V_s is −55.8 ± 3 mV and k is 10 ± 1 (mean ± SD, n = 5).

For WT channels we find that the midpoint voltage of slow inactivation is more positive than that for fast inactivation: V_s (−60.5 mV) is 7 ± 3 mV (n = 16) more positive than V_h (−68.0 mV, measured with 50-ms inactivating prepulses). As mentioned above, in both native rat (Ruff et al., 1987) and human (Ruff and Whittlesey, 1992) muscle tissue the opposite relationship has been observed, with V_s 10–25 mV more negative than V_h. In an effort to understand this difference, we investigated the possible effect of recording conditions on slow inactivation. For most of the experiments described here fluoride was the main intracellular anion. Similar results, for both WT and rT698M, were found with chloride as the intracellular anion. Slow inactivation was incomplete for rT698M currents when chloride was used, with 28 ± 12% (n = 6) of the current available at −20 mV after a 10-ms recovery pulse compared with 3.0 ± 0.4% (n = 4) for WT currents. For WT currents recorded with chloride V_s was 9 ± 2 mV (n = 4) more positive than V_h (measured with 50-ms prepulses). To examine the possibility that intracellular dialysis might shift the voltage dependence of slow inactivation relative to fast inactivation, we also measured the WT h_∞ and s_∞ curves for macroscopic currents in cell-attached patches on otherwise intact cells. In this configuration V_s was 8 ± 2 mV (n = 4) more positive than V_h. Thus the discrepancy from earlier reports does not seem to be explained by the particular recording conditions used here. Because we are expressing only the α subunit, it is possible that the β subunit plays a role in modulating slow inactivation. Interestingly, the voltage dependence of slow inactivation is more negative in fast-twitch than in slow-twitch skeletal muscle fibers (Ruff et al., 1987), indicating that slow inactivation can be affected by cellular properties.

Recovery from slow inactivation

In Fig. 2 *D* the rate of recovery for cells expressing rT698M channels appears similar to that for cells expressing WT channels. The time constant for recovery, fitted from 5 s to 5 min at −100 mV for channels inactivated at −20 mV, was actually slightly slower for rT698M (57 ± 22 s, n = 10) than for WT (39 ± 10 s, n = 9) channels ($p < 0.04$). However, recovery from slow inactivation in these experiments started with a larger fraction of current for cells expressing rT698M (Fig. 2 *D*), and the results shown in Fig. 4 *B* indicate that some of the rT698M current recovers on a time scale of milliseconds.

To investigate the speed of recovery more thoroughly, we used a protocol that measured its full time course. The recovery protocol required ~45 min to complete and had two phases: short recovery times were obtained with individual recovery pulses and long recovery times were obtained in a continuous recording. After establishing whole-cell recording, we allowed the cells to stabilize for at least 20 min at −100 mV before the peak current was measured. The cells were then held at −20 mV for at least 15 min to allow inactivation to reach a steady-state equilibrium before we started the first phase of the protocol. Once every 50 s the cells (still being held at −20 mV) were given a variable-duration recovery pulse (always at −100 mV) followed by a 20-ms test pulse (always to −10 mV). 20–25 different recovery pulse durations ranging from 1 to 500 ms were used with each cell. After the last of these, the cell was held at −20 mV for another 50 s, after which the holding potential was switched to −100 mV and recovery was measured by occasional test pulses: at 0.5-s intervals for 10 s, then at 5-s intervals for 110 s, and finally at 15-s intervals for 5 min. In this way a complete recovery profile from 1 ms to more than 7 min was obtained.

In Fig. 5 *A* the results of this protocol are shown for a cell expressing WT channels and a cell expressing rT698M channels. On this time scale it can be seen that recovery for both cells starts with close to zero current, but the initial recovery for the rT698M cell is too rapid to be resolved.

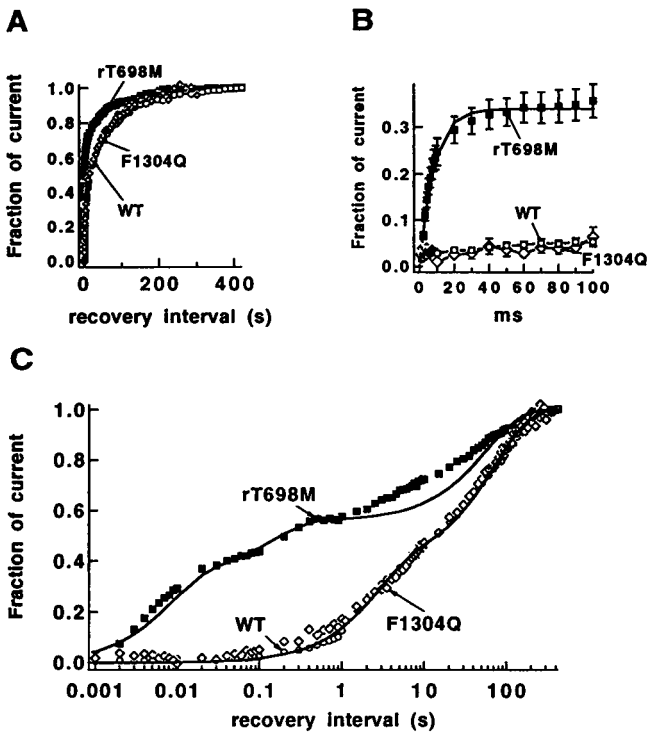

FIGURE 5 Kinetics of recovery from slow inactivation. (*A*) Normalized sodium current in representative rT698M (■), WT (○), and F1304Q (◇) cells recovering from slow inactivation (see text for protocol). (*B*) Kinetics of recovery from −20 mV with short recovery pulses for rT698M (■, n = 9), WT (○, n = 8), and F1304Q (◇, n = 5) currents. The curve through the rT698M data points is an exponential function with a time constant of 8.1 ms. (*C*) Same data as in (*A*) but with a logarithmic time axis. The curve superimposed upon the WT data points is a double exponential function (τ_1 = 2.5 s, fraction = 0.39; τ_2 = 71 s, fraction = 0.61). The rT698M curve is a triple exponential function (τ_1 = 8 ms, fraction = 0.35; τ_2 = 147 ms, fraction = 0.21; τ_3 = 57 s, fraction = 0.44). Additional exponential components would be necessary for an adequate fit of the time courses at long times.

In Fig. 5 *B* the first 100 ms of recovery is shown in detail. With recovery pulses of less than 10 ms there is almost no current (<3%) observed for WT channels but a significant amount of current for rT698M channels. The initial rate of recovery for the rT698M channels from more than 15 min at −20 mV (τ = 8.6 ± 2.6 ms, n = 9, fit between 1 and 100 ms) is identical to the rate of recovery from fast inactivation (τ = 8.1 ± 2.6 ms, n = 4, measured following a 20-ms inactivating pulse). Approximately one-third of the current recovers at this rate.

The semilogarithmic plot of Fig. 5 *C* gives an overview of the recovery kinetics of the two channel types. Very little recovery of WT channels occurs with intervals less than 1 s in duration, whereas rT698M channels show 50% recovery at 1 s. The recovery time courses do not have a simple form, requiring multiple exponentials for an adequate fit. The WT data in the figure are shown fitted with two exponentials. The fit is not good for long recovery times, and a better fit could be obtained with three exponentials (time constants of 2.5, 39, and 91 s). The rT698M data are shown with a triple exponential fit. For this cell four exponentials (time constants of 8 ms, 147 ms, 5 s, and 71 s) give a better fit.

Slow inactivation in channels with defective fast inactivation

Mutations in the III-IV interdomain linker region of the sodium channel are known to affect the fast-inactivation process. We wondered whether such mutations produce effects on slow inactivation like those seen with rT698M. The IFM sequence in the III-IV linker (positions 1303–1305 in the rat μI channel) has been identified by West et al. (1992) as being crucial for fast inactivation. When these three residues are mutated to glutamines, fast inactivation is virtually removed from RIIa brain sodium channels expressed in oocytes. Unfortunately we were unable to observe sodium currents in HEK-293 cells expressing IFM-QQQ mutants in either the WT or the rT698M backgrounds, with either transient or stable transfection protocols, even when sodium channel inhibitors (tetrodotoxin, phenytoin, lidocaine) were included in the culture medium. We also tried expressing WT-F1304Q and rT698M-F1304Q channels in HEK-293 cells. We were unable to record currents in cells either transiently or stably expressing rT698M-F1304Q channels. However, WT-F1304Q channels did express, and a stable line was established. The current density in this cell line was only ~10% of that of the WT stable lines. The F1304Q current activated normally but exhibited defective inactivation, having a time constant of ~300 ms.

Slow inactivation was not impaired by the F1304Q mutation. After the cells were held at −20 mV for 5 min, only 3 ± 2% (n = 6) of the current was available for activation after a 10-ms recovery pulse; under the same conditions WT channels show essentially the same availability (4 ± 2%, n = 5). Recovery from slow inactivation for F1304Q channels was also remarkably similar to that observed for WT channels. When subjected to the two-phase recovery protocol, F1304Q channels showed almost no recovery in the first 100 ms (Fig. 5 *B*) and showed essentially the same slow recovery time course as WT (Fig. 5 *C*). Thus the effects on inactivation of the F1304Q mutation appear to be entirely distinct from the effects of the rT698M mutation.

Tests for multiple channel populations

The time course of recovery of rT698M current contains a component with a very short time constant. It is possible that this component may reflect a separate channel population or gating mode. We tested for differences in the activation voltage dependence and kinetics of the rapidly recovering component and also checked for possible effects of expression level on the amplitude of this component. We first compared channel properties when the holding potential was −20 mV versus −100 mV. Cells were initially held

at −100 mV for at least 10 min before we obtained a current–voltage (IV) relationship (Fig. 6 *A*). The cells were then held at −20 mV for at least 5 min before another IV relationship was obtained, with a 10-ms recovery pulse to −100 mV preceding each test pulse. Test pulses were given at 25-s intervals (Fig. 6 *B*). For both rT698M and WT channels the IV relationship was identical with −20 mV and −100 mV holding potentials (Fig. 6 *A*), and the extrapolated reversal potentials were similar for all four of the mean IV curves (average 70 mV; the Nernst potential for Na^+ was 68 mV). The IV curve for rT698M channels was 13–14 mV more negative than that for WT channels at both −20 and −100 mV holding potentials. The kinetics of activation and fast inactivation were not altered by holding the cells at −20 mV (Fig. 6 *C* and *D*), and this was observed for test potentials ranging from −50 to +40 mV (data not shown).

Because the current density in WT cells is typically larger than that in rT698M, we examined whether the relative amount of current remaining available at the end of the 50-s s_∞ protocol correlated with the magnitude of the peak current. The peak current for the 16 WT cells used for Fig. 3 *A* was 13.2 ± 9.6 nA, and the peak current for the 18 rT698M cells used for Fig. 3 *B* was 8.3 ± 8.6 nA. Although the means differed, there was significant overlap: the WT peak current ranged from 1.2 to 36.2 nA and the rT698M current ranged from 1.2 to 31.4 nA. In contrast, the amount of current available at the end of the 50-s s_∞ protocol (+10-mV prepulse potential) was 2.5 ± 1% for WT cells (Fig. 3 *A*) and 16 ± 6% for rT698M cells (Fig. 3 *B*). There was no overlap between WT and rT698M cells for this measure: for WT cells the range was 1–4% and for rT698M cells it was 6–26%. There was no correlation between peak current, or peak current density (peak current normalized using cell capacitance), and the amount of current remaining available at the end of the 50-s s_∞ protocol for either WT or rT698M cells.

DISCUSSION

We have studied the effects on slow inactivation of the mutation rT698M, one of several sodium channel mutations that have been identified as causing hyperkalemic periodic paralysis in humans. In our case the mutation was studied in rat skeletal muscle sodium channels expressed in HEK-293 cells. Dramatically altered slow inactivation was observed in two independent stable rT698M lines and was also observed in cells transiently transfected with rT698M (data not shown) but was never observed in cells expressing WT channels. The mutation has two effects on slow inactivation. First, the development of slow inactivation is almost an order of magnitude slower for rT698M channels than for WT channels. Second, the recovery from slow inactivation appears to be dramatically accelerated. Even after depolarizations lasting 30 min or more, 20–30% of rT698M chan-

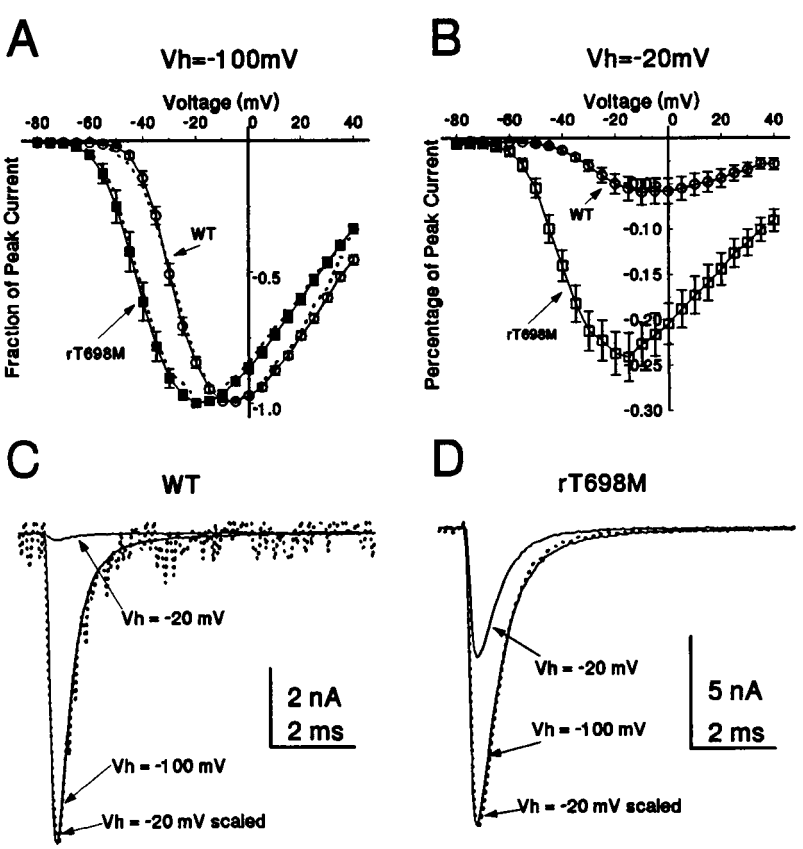

FIGURE 6 Effect of holding potential on kinetics and voltage dependence of activation. (*A* and *B*) Current voltage relationship for WT (○) and rT698M (□, ■) for depolarizations from a holding potential of −100 mV (*A*) or −20 mV following a 10-ms recovery pulse to −100 mV (*B*). The data from (*B*) are also shown scaled for comparison with the −100-mV data in (*A*) (dotted curves). The currents were elicited by 25-ms test potentials from −80 to +40 mV in 5-mV steps. For V_{hold} = −100 mV the maximum current in the WT cells was 8.3 ± 5.1 nA (n = 6); in rT698M cells, 6.5 ± 3.6 nA (n = 10). The series resistance was 2.1 ± 0.5 MΩ for WT and 1.9 ± 0.3 MΩ for rT698M cells. After series resistance compensation (80%) the estimated series resistance error for the WT data is 3 ± 2 mV and for the rT698M data is 2 ± 1 mV. Conductance-voltage (G-V) curves were calculated from these data using the equation $G_{Na} = I/(V - V_{rev})$, where G_{Na} is the fraction of conductance, I is the peak current measured, V is the test potential, and V_{rev} is the reversal potential. The G-V curves were fitted with Boltzmann functions. The midpoint and the slope for the WT G-V curve are −24.4 mV and 7.7 mV for V_{hold} = −100 mV; they are −24.0 mV and 8.4 for V_{hold} = −20 mV. For rT698M these values are −37.1 mV and 8.1 for V_{hold} = −100 mV and −37.8 and 8.3 for V_{hold} = −20 mV. (*C* and *D*) Representative current traces from a rT698M (*C*) and a WT (*D*) cell. Traces were obtained by test depolarizations to −10 mV with the holding potential shown.

nels are available for activation after a hyperpolarization lasting only 10 ms. By comparison, fewer than 3% of WT channels are available under these conditions. It is interesting to note that F1304Q mutant channels, which have impaired fast inactivation, show the same slow recovery time course as WT channels.

The rapid recovery of rT698M channels from slow inactivation could be imagined to arise in either of two ways. On the one hand, the mutation could render slow inactivation incomplete, such that 20–30% of the channels remain available after prolonged depolarizations. In this case the rapid component of recovery seen in Fig. 5 reflects the time constant of recovery from the fast-inactivation process. Alternatively, the mutation could simply speed up the slow-inactivation process. However, the rapid phase of the recovery time course would require a change in the recovery rate of 2 or 3 orders of magnitude. Regardless of the origin of the rapid recovery that is observed, the functional effect is an impairment of the slow-inactivation process, in which a substantial fraction of the channels remain readily available for activation. The impairment of slow inactivation is also reflected in the s_∞ curve for rT698M channels (Figs. 3 and 4), which cannot be well fitted with a Boltzmann function and has a much shallower voltage dependence than WT channels in either HEK-293 cells or native muscle fibers.

HyperPP patients are heterozygous for the T704M mutation. In the disorder it is believed that abnormal persistent sodium currents depolarize the muscle, resulting in inactivation of the normal sodium channels, muscle inexcitability, and paralysis. Previously it was found by ourselves (Cummins et al. 1993) and by Yang et al. (1994) that rT698M and its human counterpart, hT704M, enhance channel activation by shifting the voltage dependence of activation to more negative potentials. This shift is expected to lead to window currents, which could explain the persistent sodium currents observed in HyperPP muscle. Alternatively, it often has been proposed that in HyperPP the persistent current is caused simply by incomplete fast inactivation of the channels, and it has been observed that rT698M yields a substantial fraction of current that do not exhibit normal fast inactivation (Cannon and Strittmatter, 1993). Regardless of the origin of the persistent currents, a disruption of slow inactivation would be necessary to produce long-lasting persistent currents and to explain the extended periods of muscle weakness and paralysis that are seen in patients with HyperPP mutations (Ruff, 1994). The destabilization of slow inactivation that we report here could lead to truly persistent currents.

A direct demonstration of long-lasting persistent sodium current was unfortunately not possible in our experimental system, in part because of the relatively low level of expression of rT698M channels; the sodium current density in our cell lines was approximately one tenth of that observed in muscle fibers. Further, in our expression system the midpoint voltage of slow inactivation in the WT channel differed somewhat from that observed in native rat tissue. Therefore a definitive test of the hypothesis that impaired slow inactivation underlies HyperPP will require studies of sodium currents in the native tissue. The question also arises whether the effects reported here in the rat sodium channel might differ from those in the human channel. However, studies with the human T704M mutant channel show similar effects on slow inactivation, as will be reported elsewhere (Cummins and Sigworth, in preparation).

In addition to a possible role in the origin of prolonged depolarizing currents, altered slow inactivation might be expected to have other functional consequences. Almers et al. (1983) proposed that slow inactivation is important in the termination of myotonic discharges. Enhanced recovery from slow inactivation could account for the episodes of myotonia observed in patients with HyperPP. Ruff and Whittlesey (1992) proposed that slow inactivation is also important in the development of high-frequency muscle fatigue and might prevent injury that is due to high-frequency stimulation. Incomplete slow inactivation could increase susceptibility to cellular injury and might contribute to the myopathy that is observed in some individuals with HyperPP (McArdle, 1962).

Because the rT698M mutation both disrupts slow inactivation and enhances activation, the question arises whether the two alterations of channel function might be related. Ruben et al. (1992) presented evidence that slow inactivation in crayfish giant axons is partially coupled to activation and suggested the possibility that slow inactivation might be controlled by one of the S4 segments. The S4 segment in domain IV appears to be important in coupling activation to *fast* inactivation (Chahine et al., 1994). Might the S4 segment in domain II play a similar role for slow inactivation? This appears unlikely, because mutations scattered throughout domains II, III, and IV of the μI sodium channel have also been identified as causing HyperPP or paramyotonia congenita (Barchi 1995). It will however be interesting to see whether slow inactivation is altered by any of these other mutations.

We thank Dr. E. Marban for the F1304Q cDNA and Drs. J. F. Potts and W. S. Agnew for help with the expression constructs. This research was supported by National Institutes of Health grant NS21501 to F.J.S. This research forms part of a doctoral thesis by T.R.C.

REFERENCES

Almers, W., P. R. Stanfield, and W. Stühmer. 1983. Slow changes in currents through sodium channels in frog muscle membrane. *J. Physiol.* 339:253–271.

Barchi, R. L. 1995. Molecular pathology of the skeletal muscle sodium channel. *Annu. Rev. Physiol.* 57:355–385.

Cannon, S. C., and S. M. Strittmatter. 1993. Functional expression of sodium channel mutations identified in families with periodic paralysis. *Neuron.* 10:317–326.

Chahine, M., A. L. George, M. Zhou, S. Ji, W. Sun, R. L. Barchi, and R. Horn. 1994. Sodium channel mutations in paramyotonia congenita uncouple inactivation from activation. *Neuron.* 12:281–294.

Cummins, T. R., J. Zhou, F. J. Sigworth, C. Ukomadu, M. Stephan, L. J. Ptacek, and W. S. Agnew. 1993. Functional consequences of a Na^+ channel mutation causing hyperkalemic periodic paralysis. *Neuron.* 10: 667–668.

Fahlke, Ch., and R. Rüdel. 1992. Giga-seal formation alters properties of sodium channels of human myoballs. *Pflügers Arch.* 420:248–254.

Hodgkin, A. L., and A. F. Huxley. 1952. The dual effect of membrane potential on sodium conductance in the giant axon of *Loligo*. *J. Physiol.* 116:497–506.

Kirsch, G. E., and M. F. Anderson. 1986. Sodium channel kinetics in normal and denervated rabbit muscle membrane. *Muscle Nerve.* 9:738–747.

Lehmann-Horn, F., G. Küther, K. Ricker, P. Grafe, K. Ballanyi, and R. Rüdel. 1987. Adynamia episodica hereditaria with myotonia: a non-inactivating sodium current and the effect of extracellular pH. *Muscle Nerve.* 10:363–374.

Lehmann-Horn, F., R. Rüdel, K. Ricker, H. Lorkovic, R. Dengler, and H. C. Hopf. 1983. Two cases of adynamia episodica hereditaria: in vitro investigation of muscle cell membrane and contraction parameters. *Muscle Nerve.* 6:113–121.

McArdle, B. 1962. Adynamia episodica hereditaria and its treatment. *Brain.* 85:121–148.

Ptacek, L. J., A. L. George, R. C. Griggs, R. Tawil, R. G. Kallen, R. L. Barchi, M. Robertson, and M. F. Leppert. 1991. Identification of a mutation in the gene causing hyperkalemic periodic paralysis. *Cell.* 67:1021–1027.

Ricker, K., L. M. Camacho, P. Grafe, F. Lehmann-Horn, and R. Rüdel. 1989. Adynamia episodica hereditaria: what causes the weakness? *Muscle Nerve.* 12:883–891.

Rüdel, R., and F. Lehmann-Horn. 1985. Membrane changes in cells from myotonia patients. *Physiol. Rev.* 65:310–356.

Rüdel, R., K. Ricker, and F. Lehmann-Horn. 1993. Genotype-phenotype correlations in human skeletal muscle sodium channel diseases. *Arch. Neurol.* 50:1241–1248.

Ruben, P. C., J. G. Starkus, and M. D. Rayner. 1992. Steady-state availability of sodium channels: interactions between activation and slow inactivation. *Biophys. J.* 61:941–955.

Rudy, B. 1978. Slow inactivation of the sodium conductance in squid giant axons: pronase resistance. *J. Physiol.* 283:1–21.

Ruff, R. L. 1994. Slow Na^+ channel inactivation must be disrupted to evoke prolonged depolarization-induced paralysis. *Biophys. J.* 66:542.

Ruff, R. L., L. Simoncini, and W. Stühmer. 1987. Comparison between slow sodium channel inactivation in rat slow- and fast-twitch muscle. *J. Physiol.* 383:339–348.

Ruff, R. L., and D. Whittlesey. 1992. Na^+ current densities and voltage dependence in human intercostal muscle fibres. *J. Physiol.* 458:85–97.

Simoncini, L., and W. Stühmer. 1987. Slow sodium channel inactivation in rat and fast-twitch muscle. *J. Physiol.* 383:327–337.

Streib, E. W. 1987. AAEE minimonograph #27. Differential diagnosis of myotonic syndromes. *Muscle Nerve.* 10:603–615.

Ukomadu, C., J. Zhou, F. J. Sigworth, and W. S. Agnew. 1992. μI Na^+ channels expressed transiently in human embryonic kidney cells: biochemical and biophysical properties. *Neuron.* 8:663–676.

West, J. W., D. E. Patton, T. Scheuer, Y. L. Wang, A. L. Goldin, and W. A. Catterall. 1992. A cluster of hydrophobic amino acid residues required for fast Na^+ channel inactivation. *Proc. Natl. Acad. Sci. USA.* 89:910–914.

Yang, N., S. Ji, M. Zhou, L. J. Ptacek, R. L. Barchi, R. Horn, and A. L. George. 1994. Sodium channel mutations in paramyotonia congenita exhibit similar biophysical phenotypes in vitro. *Proc. Natl. Acad. Sci. USA.* 91:12,785–12,789.